Journal of Applied Physics

Investigation of structural changes in chiral magnet $Cr_{1/3}NbS_2$ under application of pressure

Cite as: J. Appl. Phys. **117**, 183904 (2015); https://doi.org/10.1063/1.4919833
Submitted: 15 April 2015 . Accepted: 27 April 2015 . Published Online: 12 May 2015

M. Mito, T. Tajiri, K. Tsuruta, H. Deguchi, J. Kishine, K. Inoue, Y. Kousaka, Y. Nakao, and J. Akimitsu

View Online Export Citation CrossMark

ARTICLES YOU MAY BE INTERESTED IN

Role of structural factors in formation of chiral magnetic soliton lattice in $Cr_{1/3}NbS_2$
Journal of Applied Physics **116**, 133901 (2014); https://doi.org/10.1063/1.4896950

Crystal and magnetic structures of $Cr_{1/3}NbSe_2$ from neutron diffraction
Journal of Applied Physics **119**, 013903 (2016); https://doi.org/10.1063/1.4939558

Spin structure of the anisotropic helimagnet $Cr_{1/3}NbS_2$ in a magnetic field
Applied Physics Letters **105**, 072405 (2014); https://doi.org/10.1063/1.4893567

AIP Publishing

© 2015 AIP Publishing LLC.

Investigation of structural changes in chiral magnet $Cr_{1/3}NbS_2$ under application of pressure

M. Mito,[1,a)] T. Tajiri,[2] K. Tsuruta,[1] H. Deguchi,[1] J. Kishine,[3] K. Inoue,[4,5,6] Y. Kousaka,[4,6] Y. Nakao,[7] and J. Akimitsu[4,6,7]

[1]*Graduate School of Engineering, Kyushu Institute of Technology, Kitakyushu 804-8550, Japan*
[2]*Faculty of Science, Fukuoka University, Fukuoka 814-0180, Japan*
[3]*Graduate School of Arts and Sciences, The Open University of Japan, Chiba 261-8586, Japan*
[4]*Graduate School of Science, Hiroshima University, Higashihiroshima 739-8526, Japan*
[5]*Institute for Advanced Materials Research, Hiroshima University, Higashihiroshima 739-8526, Japan*
[6]*Center for Chiral Science, Hiroshima University, Higashihiroshima 739-8526, Japan*
[7]*Department of Physics and Mathematics, Aoyama Gakuin University, Sagamihara 229-8558, Japan*

(Received 15 April 2015; accepted 27 April 2015; published online 12 May 2015)

We perform structural analysis experiments on the chiral magnet $Cr_{1/3}NbS_2$, in which Cr^{3+} ions are inserted between hexagonal NbS_2 layers. The noncentrosymmetrical nature of the inserted Cr^{3+} appears as a distorted CrS_6 octahedron. Under the application of hydrostatic pressure, the lattice shrinks significantly along the *c*-axis rather than the *a*-axis. However, at a pressure *P* of approximately 3–4 GPa, a kink in the rate of decrease in the lattice parameters is observed, and the slight movement of a Nb atom along the *c*-axis brings about a decrease in the distortion of the CrS_6 octahedron. This structural change qualitatively suggests a decrease in the strength of the Dzyaloshinskii-Moriya (D-M) interaction. Under hydrostatic pressure, the magnetic ordering temperature T_C decreases, and dT_C/dP exhibits a slight change at around 3 GPa. A series of experiments indicates that the change in the structural symmetry of the CrS_6 octahedron influences the exchange network between Cr^{3+} ions as well as the D-M interaction. © *2015 AIP Publishing LLC*. [http://dx.doi.org/10.1063/1.4919833]

I. INTRODUCTION

In a series of magnetic crystals belonging to a chiral space group without any rotoinversion symmetry elements, crystallographic chirality allows the asymmetric Dzyaloshinskii–Moriya (D–M) interaction that stabilizes either left-handed or right-handed magnetic structures.[1,2] In such a magnetic structure, whose magnetism is called chiral helimagnetism, the spin structure of the ordered state is twisted owing to the D–M interaction. When a magnetic field is applied perpendicular to the chiral axis, a periodic array of domain walls, called the chiral soliton lattice (CSL), is stabilized.[3] This coherent state is a superlattice structure, the length of which can be controlled by applying magnetic fields.[4,5] In $Cr_{1/3}NbS_2$, Togawa *et al.* observed the formation of a chiral soliton lattice through Lorenz microscopy and small-angle electron diffraction.[6] From the viewpoint of electrical conductivity, $Cr_{1/3}NbS_2$ is a metal. It exhibits magnetoresistance due to CSL formation.[7] Such a correlation between the magnetic properties and electronic transport in $Cr_{1/3}NbS_2$ can be exploited for realizing electronic devices using the macroscopic coherence of the spin phase.

From the viewpoint of crystallography, in $Cr_{1/3}NbS_2$, Cr^{3+} ions are inserted between hexagonal NbS_2 layers. The inserting of Cr^{3+} does not allow for inversion symmetry, so that the compound crystallizes as the noncentrosymmetric hexagonal space group $P6_322$.[8–10] The structure depends on how Cr^{3+} is inserted between the NbS_2 layers, which leads to changes in the electronic transport and magnetic properties.[11,12] The magnetism mainly originates from Cr^{3+} inserted in octahedral holes (2d sites), and the electronic transport from Nb (designated Nb1 and Nb2 based on the sites the atoms occupy) with two inequivalent sites (2a and 4f sites). On the other hand, sulfur atoms occupy the general position. As shown in Fig. 1, one Cr atom and three S atoms form a triangular pyramid, and the location of the Nb2 atom is such that it can occupy the central space of the inverse triangular pyramid. Two CrS_3 triangular pyramids share one Cr atom, and one triangular pyramid rotates in the direction opposite to the other around their central axis, thereby resulting in a "distorted CrS_6 octahedron." Thus, the magnetic-origin Cr is structurally correlated with the metallic-origin Nb, and the noncentrosymmetrical nature of Cr^{3+} can be evaluated via the magnitude of the distortion of the CrS_6 octahedron. Furthermore, we can also discuss its effect through changes in the position of Nb2. Recently, it has been theoretically suggested that the hybridization of the Cr orbital with the Nb orbital is important for understanding the magnetic characteristics of $Cr_{1/3}NbS_2$.[11] The density of states (DOS) of the compound have been studied for both its nonmagnetic and magnetic states.[12] The crystal lattice of magnetic Cr comprises flat triangular planes parallel to the *ab*-plane.[13] The triangular planes are located periodically at a distance of *c*/2, with a displacement by distance of *a*/3 and *b*/3.[13] It has been experimentally verified that the *ab*-plane forms the magnetically easy plane. In theory, various exchange interaction paths along both intraplane and interplane directions have been suggested. Furthermore, according to the Lorenz

[a)]Electronic mail: mitoh@mns.kyutech.ac.jp

 © 2015 AIP Publishing LLC

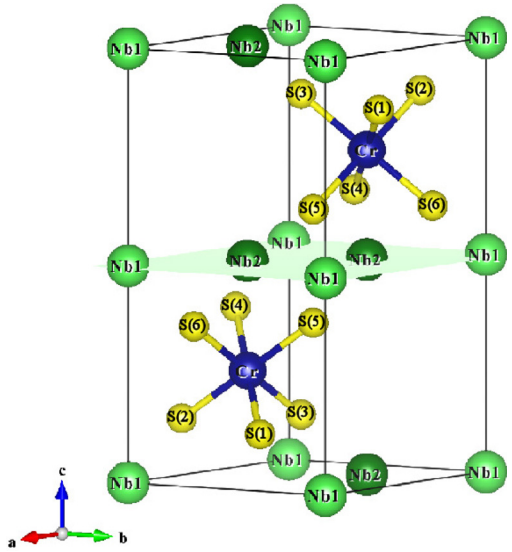

FIG. 1. Unit cell structure of $Cr_{1/3}NbS_2$. One Cr atom and three S atoms form a triangular pyramid, and the Nb atom, referred to as Nb2 (indicated in dark green), occupies the central space of the inverse triangular pyramid. The initial z-coordinate of Nb2 is 0.504. It is difficult to recognize the deviation between the z-coordinate of Nb1 (0.500) and that of Nb2 (0.504) in this figure. The x- and y-coordinates of Nb2 are the same as those of Cr. The green plane presents the (002) plane, where the Nb1 atoms with the z-coordinate of 0.500 are located. The labeling of six sulfur atoms [S(1)–S(6)] around Cr is consistent with that conducted in the inset of Fig. 5.

microscopy experiment, a ferromagnetic network develops on the *ab*-plane.[6] The decrease in the magnetic ordering temperature T_C under hydrostatic pressure was reported via the ac magnetic susceptibility measurement.[14] Thus, we think that it is important to investigate the magneto-structural correlation by conducting X-ray diffraction (XRD) analysis under hydrostatic pressure. In the present study, we investigate the crystal structure of $Cr_{1/3}NbS_2$ as a function of pressure, and we examine how the noncentrosymmetrical nature of Cr^{3+} varies with pressure.

II. EXPERIMENTAL PROCEDURES

Single crystals and powder samples of $Cr_{1/3}NbS_2$ were synthesized through a procedure described elsewhere.[6] Powder XRD analysis was conducted under hydrostatic pressures of up to 6.8 GPa at room temperature using a synchrotron radiation XRD system with a cylindrical imaging plate at the Photon Factory (PF) at the Institute of Materials Structure Science, High Energy Accelerator Research Organization (KEK).[15] The wavelength of the incident X-rays was 0.67561 Å. Pressure was applied using a diamond-anvil cell (DAC), which consisted of two diamond anvils with flat tips having a diameter of 0.8 mm and a 0.3-mm-thick CuBe gasket. The powder sample of $Cr_{1/3}NbS_2$ was contained in a sample cavity with a diameter of 0.4 mm, along with a ruby that was used as a manometer and fluorinated oil as the pressure-transmitting medium. The magnitude of pressure (P) was estimated by measuring the fluorescence of the ruby.[16] The diffraction patterns obtained under pressure application were analyzed by means of the Rietveld refinement using the RIETAN-2000 package.[17]

The in-phase ac magnetic susceptibility (χ') of the single crystal was observed using a superconducting quantum interference device (SQUID) magnetometer (Quantum Design, Inc.) equipped with an ac measurement option. The frequency and amplitude of the ac field were 10 Hz and 4 Oe, respectively. The ac field H_{ac} was applied parallel to the easy plane, *ab*-plane (i.e., $H_{ac} \perp c$-axis), so as to detect a sufficient magnetic response even in experimental situations requiring a minute sample volume. The pressure for the magnetic measurement was obtained by using a miniature DAC (mDAC) for $P \leq 6.0$ GPa,[18] which was designed to be inserted into the SQUID magnetometer. The culet size of the diamond anvils was 1.0 mm, and the thickness of the CuBe gasket was 0.2 mm. The single crystal of $Cr_{1/3}NbS_2$ was contained in a sample cavity with a diameter of 0.5 mm, along with a ruby that was used as a manometer[16] and Apiezon-J oil as the pressure-transmitting medium.

III. EXPERIMENTAL RESULTS

A. X-ray diffraction

Figure 2 shows the corresponding XRD patterns of $Cr_{1/3}NbS_2$ at representative pressures applied in the sequence of $0 \rightarrow 6.8 \rightarrow 0 \rightarrow 2.1$ GPa. The XRD pattern at ambient pressure is fitted with the lattice parameters corresponding to the crystal structure of $P6_322$. As the pressure increases, the diffraction pattern reflecting the structural symmetry of C_6 shifts toward higher angles. As pressure increases, each diffraction peak becomes broader due to the increase in the strain: The strain at $P = 0$ GPa (10) and 2.1 GPa (12) is almost the same as that at $P = 4.5$ GPa (6) and 6.8 GPa (9), respectively. The analytic results for the data after releasing pressure of 6.8 GPa should not be compared with the systematic changes of the structural parameters obtained for the data in the first process of ascending pressure. The R_F values for $P = 0$ GPa (1) and 6.8 GPa (9) are 4.04 ($R_{wp} = 7.81$, $R_e = 4.19$) and 4.71 ($R_{wp} = 8.00$, $R_e = 4.23$), which are lower than the permissible level of 5.0.[19] At $P = 0$ GPa (1), $a = 5.7121 \pm 0.0002$ Å and $c = 12.0542 \pm 0.0005$ Å, and at $P = 6.8$ GPa (9), $a = 5.6477 \pm 0.0006$ Å and $c = 11.7737 \pm 0.0019$ Å. Thus, the Rietveld analysis for each XRD pattern has converged in an authentic level, whereas the effective error appears especially in the atomic coordinate of light sulfur atom. A series of pattern-fitting analyses yielded the pressure dependences of the lattice constants, as presented in Fig. 3. Here, V denotes the volume of the unit cell. However, this increase in the error bar does not obstruct observation of the systematic change in a, c, and V in Fig. 3. The contraction ratio along the c-axis is approximately twice that along the a-axis, and this tendency is consistent with the preliminary results of the first principles calculation.[20] At approximately 3 GPa, a kink in the rate of decrease is observed in the pressure dependences of a, c, and V. Further detailed analysis also yielded the atomic positions of Nb2 and S located at their general positions, as shown in Fig. 4. The z-coordinates of Nb2 begin to exhibit a large change at around 3 GPa, and they eventually approach the value of 0.5, which is the z-coordinate of Nb1. The latter behavior has also been inferred from the first-principles calculation.[20] This behavior exhibited by the z-coordinates of Nb2 suggests that, initially, the Nb2-plane is far from the Nb1-plane (located in the special position); however, under

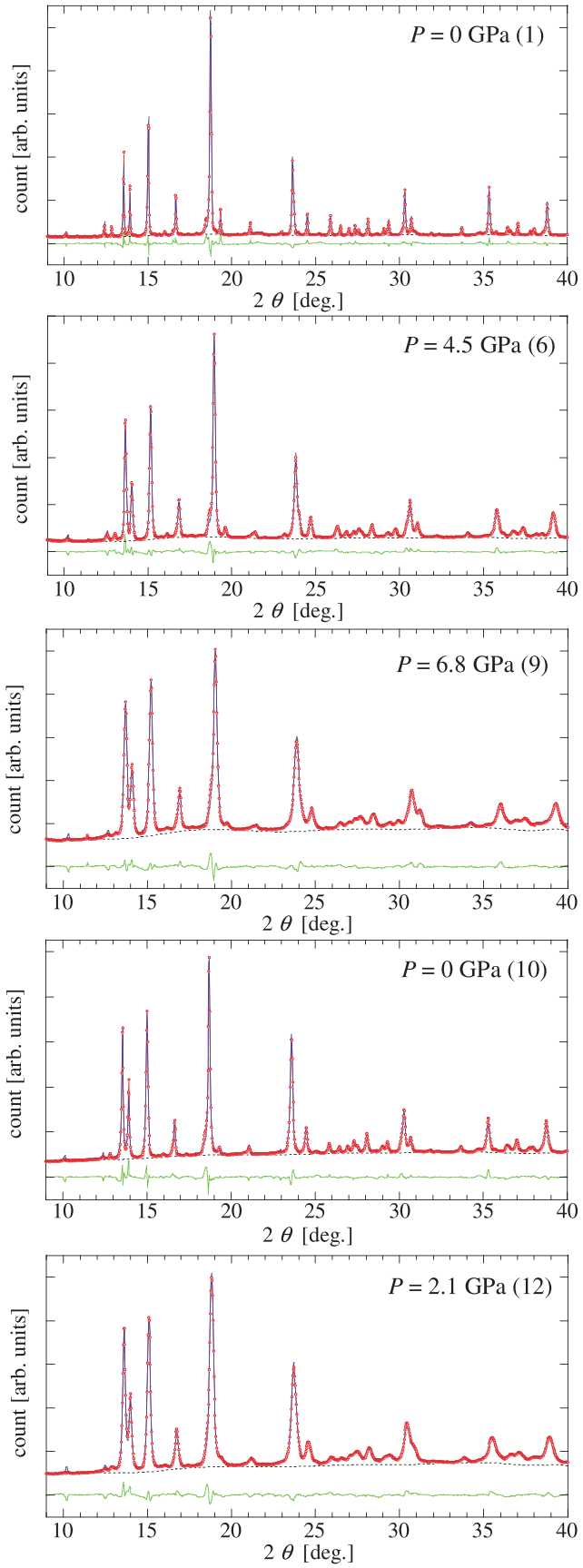

FIG. 2. XRD patterns of $Cr_{1/3}NbS_2$ at pressures up to 6.8 GPa. Red, blue, black, and green curves indicate experimental data, analytic data for fitting, background, and deviation between experimental and analytic data, respectively. The number in parentheses after the pressure value indicates the sequence of measurements under pressures.

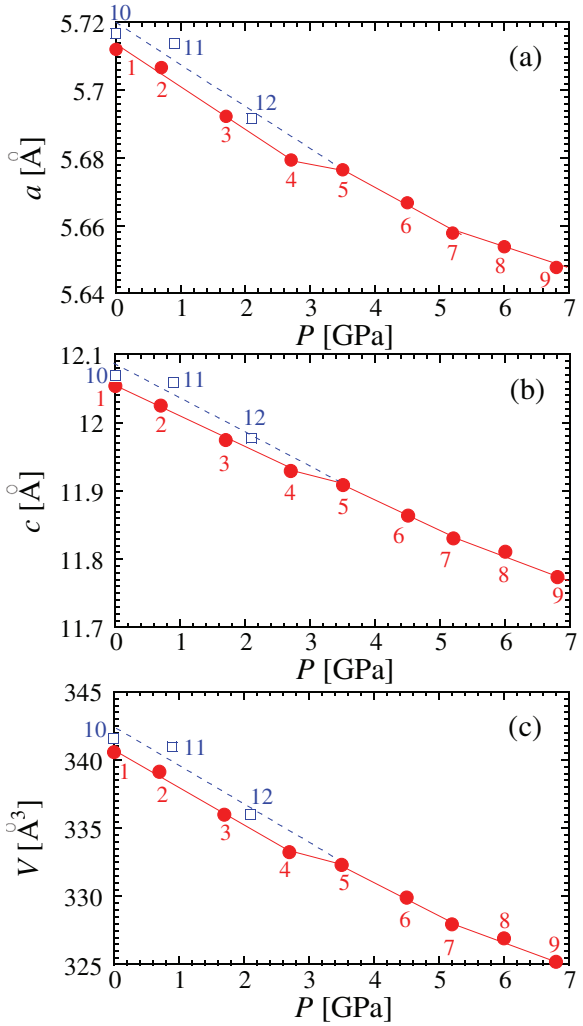

FIG. 3. Pressure dependences of the lattice constants (a and c) and the unit cell volume V of $Cr_{1/3}NbS_2$ at pressures up to 6.8 GPa. The numbers indicate the sequence of the measurements. The error bar in the estimation of lattice constants using Rietveld analysis is smaller than the size of each symbol.

high pressure, the Nb2-plane eventually overlaps with the Nb1-plane. In our experiment, this reordering continues even after the pressure is released at 6.8 GPa, thereby qualitatively indicating that a new structure is formed at ambient pressure. The estimation error of pressure is less than 0.2 GPa. Even if there would be residual stress after releasing $P = 6.8$ GPa, the expansion of the lattice constant cannot be explained. We suppose that the annealing at high pressures up to 6.8 GPa stabilizes the quasi-stable crystal structure differently from the initial structure. Here, from the viewpoint of the symmetry of the CrS_6 octahedron, the structural space group continues to exist as a chiral space group after removal of the pressure of 6.8 GPa. In contrast, the z-coordinates of S (S_z) show a systematic change as a function of P, and after the pressure is released at 6.8 GPa, the resulting value of S_z is inconsistent with its initial value. The x-coordinates of S are not reversible against releasing of pressure, whereas its y-coordinates are nearly reversible.

Figures 5(a)–5(c) show the prominent bonding angles, ∠S(5)S(1)S(6), ∠S(3)S(1)S(5), and ∠S(6)S(1)S(2), considering the apex of the octahedron S(1) as the center of the

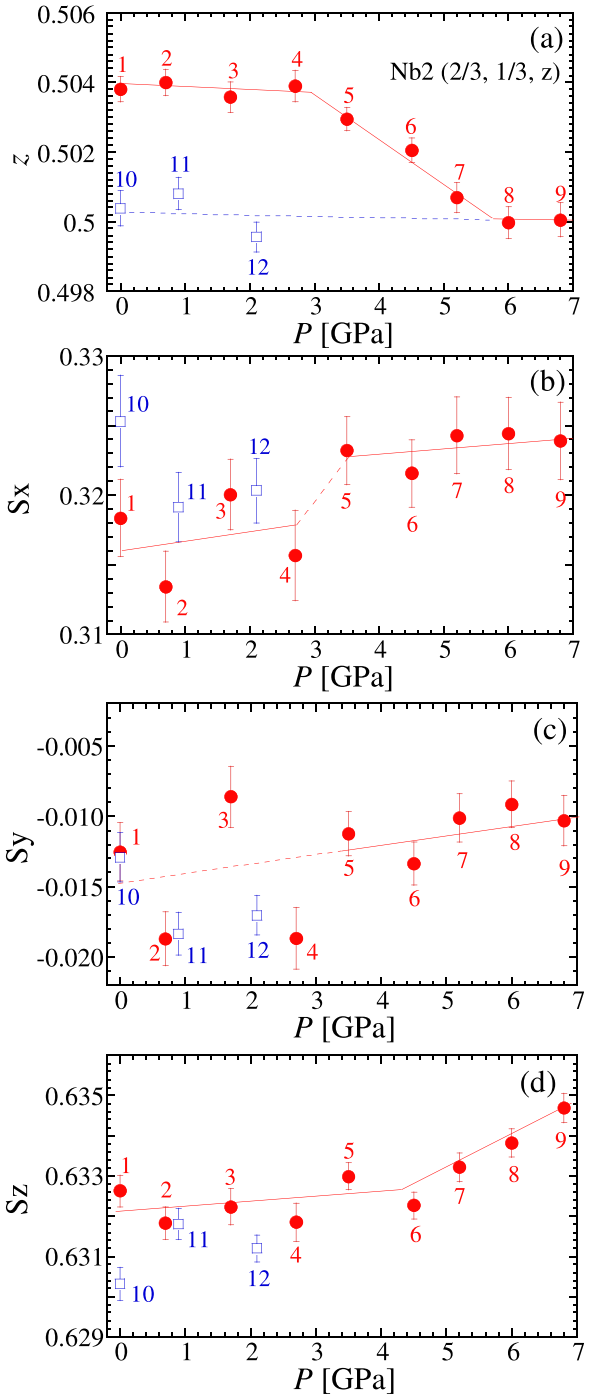

FIG. 4. Pressure dependence of atomic positions of Nb2 and S at pressures up to 6.8 GPa. All coordinates are dimensionless. The dotted lines indicate the hypothesized pressure dependence. The numbers indicate the sequence of measurements.

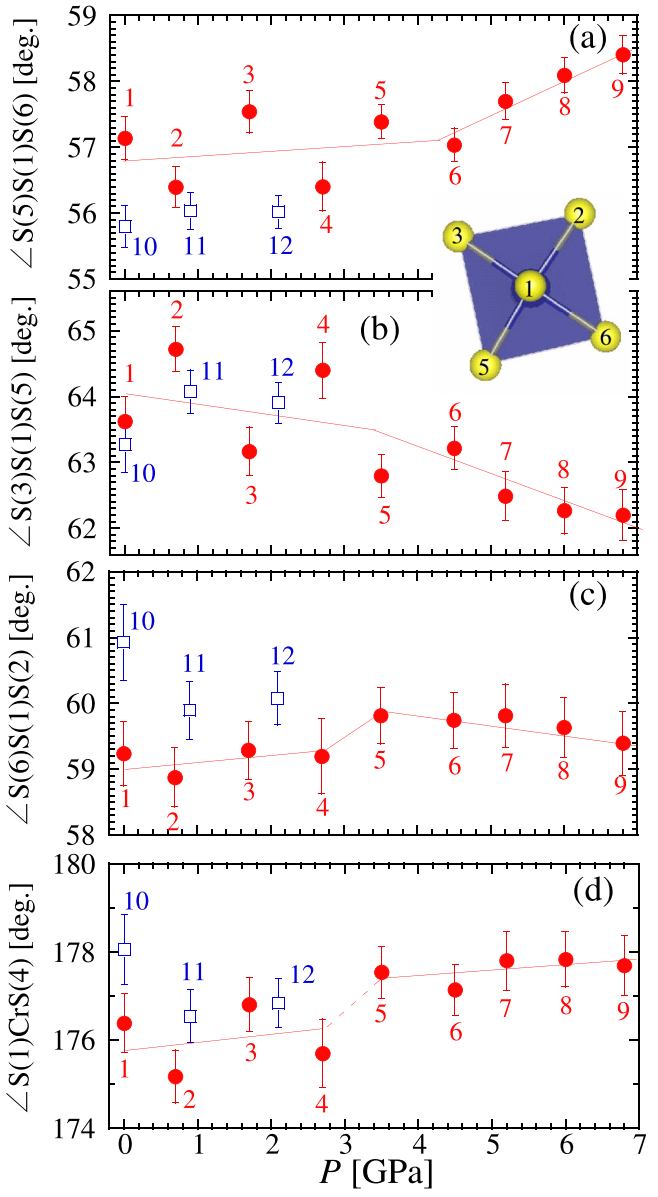

FIG. 5. Pressure dependence of primitive S–S–S angles (a)–(c) of the pyramid consisting of five sulfur atoms as S(1), S(2), S(3), S(5), and S(6) (i.e., the upper half of the CrS_6 octahedron) and the S–Cr–S angle (d) formed by the central Cr and two apical S atoms of the CrS_6 octahedron at pressures up to 6.8 GPa. The numbers indicate the sequence of measurements.

bonding angle. Here, the triangle △S(2)S(1)S(3) is a regular triangle, and ∠S(2)S(1)S(3) is always 60°. ∠S(5)S(1)S(6) and ∠S(6)S(1)S(2) exhibit no prominent reversibility after removal of the pressure of 6.8 GPa. The pressure response of ∠S(3)S(1)S(5) over the course of the application and removal of pressure is almost reversible. Thus, the resulting position of S does not revert to the initial position particularly owing to the change in *x*- and *z*-coordinates. We stress that all three abovementioned angles tend to approach 60°. This implies that the symmetry of the octahedron composed of six sulfur atoms approaches that of the regular octahedron. This feature can be observed in the pressure dependence of the S(1)–Cr–S(4) angle formed by the central Cr and the two apical S atoms of the CrS_6 octahedron, as shown in Fig. 5(d). The value of ∠S(1)CrS(4) tends to approach 180° with increasing pressure. It is natural that this change in the symmetry of the octahedron is strongly correlated with the change in the *z*-coordinates of Nb2, which is characterized as the insertion of Nb2 into the triangle formed with S(1), S(2), and S(3). It is considered that the effective *c*-axis compression induces a corresponding movement of Nb2, thereby leading to "untwisting" of the CrS_3 pyramid.

B. AC magnetic susceptibility

Figure 6 shows the temperature (T) dependence of the in-phase ac magnetic susceptibility (χ') of $Cr_{1/3}NbS_2$ for the first pressure run of $P \leq 3.1$ GPa and the second pressure run of $P \leq 6.0$ GPa. The background contribution owing to the mDAC is subtracted in both sets of figures. T_C is determined from the characteristic cusp for $H_{ac} \perp c$-axis. The value of T_C at ambient pressure is estimated to be 130 K via two runs, which is nearly consistent with the previously reported T_C value of 127 K.[10] As shown in Fig. 6, when the applied pressure increases, the cusp of χ' shifts toward the low-temperature region, thereby suggesting a systematic reduction in T_C. Furthermore, the magnitude of the ac magnetic susceptibility below T_C is inconsistent with the change in pressure, thereby suggesting that the easy-plane type of anisotropy hardly changes even under pressure. Figure 7 shows the pressure dependence of T_C, the data of which has been reported elsewhere.[14] T_C decreases nearly linearly against pressure as $dT_C/dP = -6.9$ K/GPa, whereas its decrease exhibits a small deceleration at around 3–4 GPa. At this point, the change in T_C deviates from the linear trend, which is indicated by the dotted line in Fig. 7. In our previous study, we did not focus on this deceleration of T_C at around 3–4 GPa. The existence of a characteristic pressure range has already been suggested in the structural data, as discussed in the Sec. III A. As seen in Fig. 6(a), after the removal of the pressure of 3.1 GPa, T_C exhibits a value higher than the initial one, thereby suggesting that a new modified exchange network is stabilized by the one-time application of a pressure of about 3 GPa. This irreversibility is consistent with the structural irreversibility after releasing the pressure of 6.8 GPa, as mentioned in Sec. III A. The irreversibility accompanying the increase in T_C was also observed in the ac magnetic susceptibility measurement of the powder sample in the preliminary experiment at pressures up to 13.5 GPa, wherein reversibility was observed for $P \leq 1.3$ GPa. We assume that the irreversibility observed in both the structural parameters and T_C occurs after the sample experiences a characteristic pressure of approximately 3 GPa.

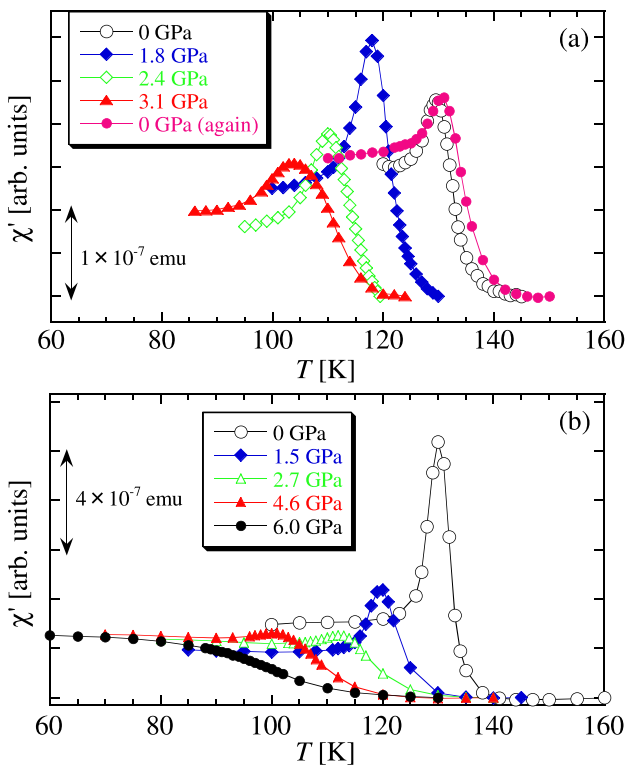

FIG. 6. In-phase ac magnetic susceptibility χ' of $Cr_{1/3}NbS_2$ under various pressures: (a) the first run for the pressure increase sequence of 0 → 3.1 GPa, and after removal of 3.1 GPa, and (b) the second run for the pressure increase sequence of 0 → 6.0 GPa.

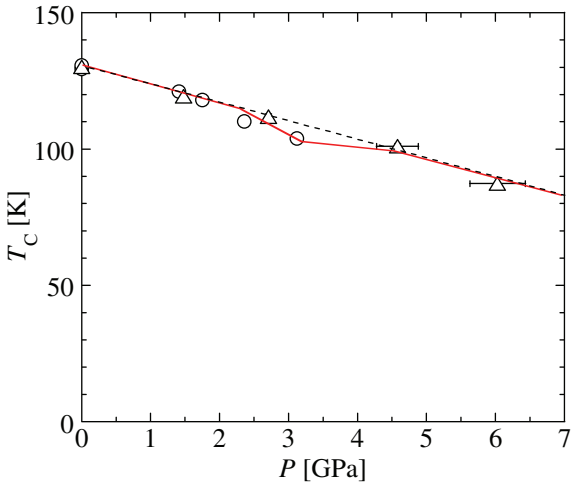

FIG. 7. Pressure dependence of T_C of $Cr_{1/3}NbS_2$ estimated from the characteristic anomaly in χ' for $Cr_{1/3}NbS_2$ [(○) the first run, (△) the second run]. The dotted straight line represents the plot of T_C [K] = 129.9 − 6.9 × P [GPa].

IV. DISCUSSION

In this section, we discuss how the noncentrosymmetrical nature of Cr^{3+} accompanying the distortion of the CrS_6 octahedron works to stabilize the chiral magnetic ordering in $Cr_{1/3}NbS_2$ via the results of the artificial structure-manipulation under pressure. We focus on determining a significant correlation between the change in T_C and the structural change as a function of pressure, since both the structural parameters and T_C exhibit the kink in the rate of decrease at around 3–4 GPa. Furthermore, it has been known that this material exhibits a large nonlinear magnetic response under an ac field. At around 3 GPa, the cusp of the third-order harmonic susceptibility and that of the first-order harmonic susceptibility begin to deviate from each other.[14] The present structural data indicates that at around 3–4 GPa, the local structural symmetry begins to change prominently, suggesting the existence of a magneto-structural correlation.

Below, we explain the change in the noncentrosymmetrical nature of Cr^{3+} in detail. The Cr and Nb1 atoms are located in the special position, and therefore we focus on the change in the positions of S and Nb2. First, the unit cell tends to shrink along the c-axis prominently, whereas both a and c exhibit a change in the slopes of their pressure dependences at around 3–4 GPa. The change in the position of S atoms induces a suppression of the distortion of the CrS_6 octahedra. The structural symmetry of CrS_6 is related to the D–M interaction, and the change reported in this study

qualitatively suggests a reduction in the strength of the D–M interaction (D) with increasing pressure. For instance, an examination of the crystal structure data at $P = 6.8$ GPa suggests that Nb1 and Nb2 share the same *ab*-plane, and in this case, the distortion of CrS_6 is almost absent; we suppose that D becomes quite small.

The change in the distortion of CrS_6 influences the exchange network between Cr^{3+} ions.[13] The magnetic network of $Cr_{1/3}NbS_2$ is considered to be a two-dimensional Heisenberg system,[6,13] and consequently T_C is a function of both the correlation length on the *ab*-plane, ξ_{2D} (T), at $T = T_C$ and the interplane interaction along the *c*-axis, J' as

$$k_B T_c \propto J' S^2 \xi_{2D}^2 (T = T_C), \quad (1)$$

where S denotes the spin quantum number and ξ_{2D} $(T = T_C)$ is related to the intraplane interaction on the *ab*-plane, J_{2D}.[21] Thus, T_C is a function of the square of ξ_{2D} $(T = T_C)$. The Monte Carlo simulation results for the evaluation of T_C in $Cr_{1/3}NbS_2$ indicate that T_C prominently depends on J_{2D}.[22] T_C estimated by the first-order harmonic susceptibility significantly decreases with the slope of $dT_C/dP = -6.9$ K/GPa, and the change in T_C is supposed to be governed by the change in J_{2D} rather than that in J'. The large change in T_C under pressure may suggest the importance of itinerant electrons on the magnetic network. It remains a future work to study how the change in the position of S is related to the decrease in J_{2D}.

V. CONCLUSION

We investigated the magneto-structural correlation in $Cr_{1/3}NbS_2$ through a structural analysis experiment and ac magnetic susceptibility measurements under pressure. The structural change at the unit cell level was determined, and an increase in the symmetry of the CrS_6 octahedron was observed. This structural change indicates that the D–M interaction tends to be suppressed under pressure. In particular, at around 3–4 GPa, the distortion of the CrS_6 octahedron began to decrease ("untwist") prominently. Structurally, the suppression of the noncentrosymmetrical nature of Cr^{3+} originates mainly from lattice compression along the *c*-axis. On the other hand, the magnetic ordering temperature decreases upon application of pressure. This phenomenon indicates that the change in the structural symmetry of the CrS_6 octahedron influences the exchange network between Cr^{3+} ions as well as the D-M interaction.

ACKNOWLEDGMENTS

This work was supported by a Grant-in-Aid for Scientific Research Grant Nos. (A) 18205023 and (S) 25220803 from the Ministry of Education, Culture, Sports, Science and Technology (MEXT), Japan.

[1]I. E. Dzialoshinskii, Sov. Phys. JETP **5**, 1259 (1957).
[2]T. Moriya, Phys. Rev. **120**, 91 (1960).
[3]J. Kishine, K. Inoue, and Y. Yoshida, Prog. Theor. Phys., Suppl. **159**, 82 (2005).
[4]I. G. Bostrem, J. Kishine, and A. S. Ovchinnikov, Phys. Rev. B **77**, 132405 (2008).
[5]I. G. Bostrem, J. Kishine, and A. S. Ovchinnikov, Phys. Rev. B **78**, 064425 (2008).
[6]Y. Togawa, T. Koyama, K. Takayanagi, S. Mori, Y. Kousaka, J. Akimitsu, S. Nishihara, K. Inoue, A. S. Ovchinnikov, and J. Kishine, Phys. Rev. Lett. **108**, 107202 (2012).
[7]Y. Togawa, Y. Kousaka, S. Nishihara, K. Inoue, J. Akimitsu, A. S. Ovchinnikov, and J. Kishine, Phys. Rev. Lett. **111**, 197204 (2013).
[8]A. R. Beal, in *Intercalated Layered Materials*, edited by F. A. Levy (D. Reidel Publishing Company, Dordecht, Holland, 1979).
[9]F. Hulliger and E. V. A. Pobitschka, J. Solid State Chem. **1**, 117 (1970).
[10]T. Miyadai, K. Kikuchi, H. Kondo, S. Sakka, M. Arai, and Y. Ishikawa, J. Phys. Soc. Jpn. **52**, 1394 (1983).
[11]H. Matsuura, private communication (2014).
[12]N. J. Ghimire, M. A. McCuire, D. S. Parker, B. Sipos, S. Tang, J.-Q. Yan, B. C. Sales, and D. Mandrus, Phys. Rev. B **87**, 104403 (2013).
[13]L. M. Volkova and D. V. Marinin, J. Appl. Phys. **116**, 133901 (2014).
[14]M. Mito, S. Tominaga, Y. Komorida, H. Deguchi, S. Takagi, Y. Nakao, Y. Kousaka, and J. Akimitsu, J. Phys.: Conf. Ser. **215**, 012182 (2010).
[15]A. Fujiwara, K. Ishii, T. Watanuki, H. Suematsu, H. Nakao, K. Ohwada, Y. Fujii, Y. Murakami, T. Mori, H. Kawada, T. Kikegara, O. Shimomura, T. Matsubara, H. Hanabusa, S. Daicho, S. Kitamura, and C. Katayama, J. Appl. Crystallogr. **33**, 1241 (2000).
[16]G. J. Piermarini, S. Block, J. D. Barnett, and R. A. Forman, J. Appl. Phys. **46**, 2774 (1975).
[17]F. Izumi and T. Ikeda, Mater. Sci. Forum **321–3**, 198 (2000).
[18]M. Mito, M. Hitaka, T. Kawae, K. Takeda, T. Kitai, and N. Toyoshima, Jpn. J. Appl. Phys., Part **1 40**, 6641 (2001).
[19]R. A. Young, *The Rietveld Method*, edited by R. A. Young (Oxford University Press, Oxford, 1993).
[20]T. Shishido, private communication (2014).
[21]M. Mito, H. Nakano, T. Kawae, M. Hitaka, S. Takagi, H. Deguchi, K. Suzuki, K. Mukai, and K. Takeda, J. Phys. Soc. Jpn. **66**, 2147 (1997).
[22]M. Shinozaki, S. Hoshino, J. Kishine, K. Hukushima, and Y. Kato, in Japan-Russia International Research Symposium on Chiral Magnetism, Hiroshima, Japan, 6–8 December 2014, Abstract O05.